π-Arene Aqua Complexes of Cobalt, Rhodium, Iridium, and Ruthenium: Preparation, Structure, and Kinetics of Water Exchange and Water Substitution†

Lynda Dadci,[1a] Horst Elias,*[,1b] Urban Frey,[1a] Andreas Hörnig,[1c] Ulrich Koelle,*[,1c] André E. Merbach,*[,1a] Helmut Paulus,[1d] and Jens Stefan Schneider[1b]

Eduard-Zintl-Institut für Anorganische Chemie, Technische Hochschule Darmstadt, D-64289 Darmstadt, Germany, Institut de Chimie Minérale et Analytique, Université de Lausanne, BCH, CH-1005 Lausanne, Switzerland, and Institut für Anorganische Chemie, Technische Hochschule Aachen, D-52065 Aachen, Germany

Received June 8, 1994[⊗]

The half-sandwich complexes $[Cp^*Co(bpy)(H_2O)](PF_6)_2$, $[Cp^*M(bpy)Cl]Cl$ (M = Rh, Ir), $[L^{2-4}Ru(bpy)Cl]Cl$, and $[Cp^*Ir(OH)_3IrCp^*]OH\cdot 11H_2O$ were prepared and characterized ($Cp^* = L^1 = \eta^5$-pentamethylcyclopentadienyl anion; bpy = 2,2′-bipyridine; $L^2 = \eta^6$-benzene; $L^3 = \eta^6$-cymene; $L^4 = \eta^6$-hexamethylbenzene). X-ray structure analyses of $[Cp^*Rh(bpy)Cl]ClO_4$ (=$C_{20}H_{23}Cl_2N_2O_4Rh$; orthorhombic, $Pmn2_1$; a = 12.720(5), b = 8.141(5), c = 10.504(5) Å; Z = 2; R_w = 0.0352), $[Cp^*Ir(bpy)Cl]ClO_4$ (=$C_{20}H_{23}Cl_2IrN_2O_4$; orthorhombic, $Pmn2_1$; a = 12.714(4), b = 8.216(4), c = 10.507(4) Å; Z = 2; R_w = 0.0235), and $[Cp^*Ir(OH)_3IrCp^*]OH\cdot 11H_2O$ (=$C_{20}H_{56}Ir_2O_{15}$; orthorhombic, *Pnma*; a = 17.43(2), b = 17.93(2), c = 10.52(1) Å; Z = 4; R_w = 0.0317) were carried out. Complexes $[Cp^*Rh(bpy)Cl]ClO_4$ and $[Cp^*Ir(bpy)Cl]ClO_4$ are isostructural. The dinuclear triply OH-bridged complex $[Cp^*Ir(OH)_3IrCp^*]OH\cdot 11H_2O$ is isostructural with $[Cp^*Rh(OH)_3RhCp^*]OH\cdot 11H_2O$ (Nutton et al. *J. Chem. Soc., Dalton Trans.* **1981**, 1997) with the two Cp* ligands being orientated in a coplanar fashion. The pK_a's (298 K, I = 0.5 M ($NaClO_4$)) of the coordinated water in the monoaqua species $[Cp^*M(bpy)(H_2O)]^{2+}$ were found to be 8.4 (Co), 8.2 (Rh), and 7.5 (Ir). The coordinated water in the species $[L^{2-4}Ru(bpy)(H_2O)]^{2+}$ is slightly more acidic (pK_a = 6.9 (L^2), 7.2 (L^3), 7.3 (L^4)). The vis absorption characteristics of the complex cations $[Cp^*M(bpy)X]^{2+/+}$ (M = Co, Rh, Ir) and $[L^{2-4}Ru(bpy)X]^{2+/+}$ are reported for X = H_2O, SCN, I, Br, N_3, thiourea, *N*-methylimidazole. Stopped-flow spectrophotometry was used to study the anation kinetics of the species $[Cp^*M(bpy)(H_2O)]^{2+}$ (M = Co, Rh, Ir) and $[L^{2-4}Rh(bpy)(H_2O)]^{2+}$ in aqueous solution at pH 4.8 for a variety of monodentate anionic and neutral ligands X at variable temperature. The kinetics follow a second-order rate law, rate = k_X[X][complex]. On the basis of the Eigen−Wilkins mechanism, the second-order rate constants k_X were corrected for outer-sphere complex formation to obtain the rate constants for the interchange step, k_i, according to $k_i = k_X/K_{os}$ (K_{os} was calculated). Rate constants k_i are nearly independent of the nature of the entering ligand X. The data for k_i(average) (=mean of k_i for all of the nucleophiles X studied) thus obtained range from k_i(average) = 0.068 ± 0.038 s^{-1} for $[L^2Ru(bpy)(H_2O)]^{2+}$ to k_i(average) = 1590 ± 760 s^{-1} for $[Cp^*Rh(bpy)(H_2O)]^{2+}$. For the homologous series $[Cp^*M(bpy)(H_2O)]^{2+}$ (M = Co, Rh, Ir) the order for k_i(average) (s^{-1}) is found to be Co:Rh:Ir = 0.60:1590:219 at 293 K. The data obtained for k_i(average) can be taken as a good approximation for the rate of water exchange; i.e., k_i(average) = k_{ex}. ^{17}O-NMR techniques were used to study the water exchange in $[Cp^*Rh(H_2O)_3]^{2+}$ and $[Cp^*Ir(H_2O)_3]^{2+}$ at variable temperature and pressure. The kinetic data for k_{ex}^{298} (s^{-1}), $\Delta H^{\ddagger}$ (kJ mol^{-1}), $\Delta S^{\ddagger}$ (J K^{-1} mol^{-1}), and $\Delta V^{\ddagger}$ (cm^3 mol^{-1}) are 1.6 × 10^5, 65.6, +75.3, and +0.6 for $[Cp^*Rh(H_2O)_3]^{2+}$ and 2.53 × 10^4, 54.9, +23.6, and +2.4 for $[Cp^*Ir(H_2O)_3]^{2+}$. The ratio k_{ex}(Rh)/k_{ex}(Ir) for the species $[Cp^*M(H_2O)_3]^{2+}$ is very close to the ratio k_i(average)(Rh)/k_i(average)(Ir) for the species $[Cp^*M(bpy)(H_2O)]^{2+}$. The kinetic findings support the operation of an (dissociative) interchange mechanism ($I_{(d)}$) for the anation of the species $[LM(bpy)(H_2O)]^{2+}$ (M = Co, Rh, Ir; L = L^1−L^4) as well as for the water exchange in $[Cp^*M(H_2O)_3]^{2+}$ (M = Rh, Ir). The rate-enhancing effect of π-arene ligands L on the water exchange in the half-sandwich cations $[LM(H_2O)_3]^{2+}$ and $[LM(bpy)(H_2O)]^{2+}$ is discussed.

Introduction

Complex formation according to (1) is very much determined by the mobility of the coordinated solvent molecules forming

$$[MS_n]^{q+} + L \rightleftharpoons [MS_{n-1}L]^{q+} + S \qquad (1)$$

the solvation sphere of the metal ion M^{q+}. The rate of solvent exchange according to (2), as characterized by rate constant k_{ex},

$$[MS_n]^{q+} + nS^* \overset{k_{ex}}{\rightleftharpoons} [MS_n^*]^{q+} + nS \qquad (2)$$

can be taken as a measure for the "lability" or "inertness" of the solvated metal ion MS_n^{q+}. The data for k_{ex} are thus of fundamental significance, and considerable effort has been made to determine k_{ex} for a great variety of metals and solvents, to elucidate the mechanism of solvent exchange, and to set up theoretical concepts for the correlation of k_{ex} with parameters such as the charge, size, and electron configuration of M.[2]

† Dedicated to Prof. Dr. H. Schmidbaur on the occasion of his 60th birthday.

⊗ Abstract published in *Advance ACS Abstracts,* November 15, 1994.

(1) (a) Lausanne. (b) Darmstadt. (c) Aachen. (d) Darmstadt, Fachbereich Materialwissenschaft.

0020-1669/95/1334-0306$09.00/0

Chart 1

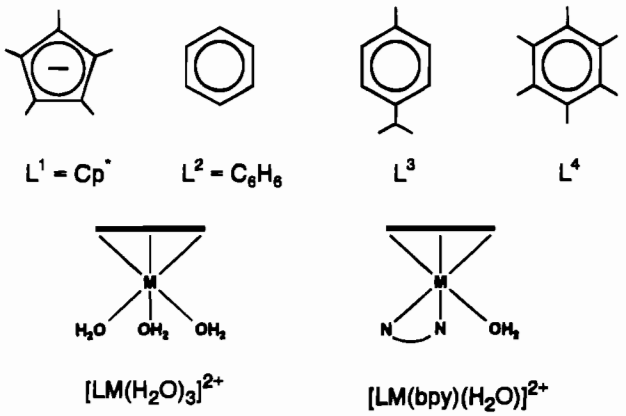

It is a well-known fact that, for a given solvated metal ion, the size of k_{ex} is affected by the nature of the solvent S and by changes in the solvation shell of M^{q+}. This means, in more general terms, that k_{ex} depends on the ligand field around the metal. Compared to that in the hexaaqua ion $Ni(H_2O)_6^{2+}$, for example, water exchanges in $Ni(H_2O)_5(NH_3)^{2+}$, $Ni(H_2O)_3(NH_3)_3^{2+}$, and $Ni(H_2O)(NH_3)_5^{2+}$ are faster by factors of about 8,[3a] 78,[3a] and 134,[3b] respectively. A similar rate enhancement is observed for water exchange in the corresponding cobalt(III) aqua amine complexes[3a] and in mononuclear and dinuclear chromium(III) aqua hydroxo complexes.[3c] On the other hand, the fact that water exchange is approximately 9 times faster in $Ni(H_2O)_4(en)^{2+}$ than in $Ni(H_2O)_4(bpy)^{2+}$ indicates that the nature of the ligands replacing the water is important too.[3a]

As exemplified by the couples $Ru(H_2O)_6^{2+}/Ru(\eta^6\text{-}C_6H_6)(H_2O)_3^{2+}$ and $Ru(CH_3CN)_6^{2+}/Ru(\eta^6\text{-}C_6H_6)(CH_3CN)_3^{2+}$, the rates of the solvent exchange in half-sandwich solvento complexes are accelerated drastically by factors of about 640 (H_2O)[4,5] and 4.6×10^5 (CH_3CN),[4,6] respectively, when a π-arene ligand such as benzene replaces three of the solvent molecules.

The present study was undertaken to contribute to the understanding of the rate enhancement of water exchange in mixed ligand–aqua complexes by an investigation of the half-sandwich aqua complexes $[L^1M(H_2O)_3]^{2+}$ = $[Cp^*M(H_2O)_3]^{2+}$ (M = Rh(III), Ir(III)), $[L^1M(bpy)(H_2O)]^{2+}$ = $[Cp^*M(bpy)(H_2O)]^{2+}$ (M = Co(III), Rh(III), Ir(III)), and $[L^{2-4}Ru^{II}(bpy)(H_2O)]^{2+}$, as formed by a variety of π-arene ligands L (see Chart 1). Direct water exchange in complexes $[Cp^*M(H_2O)_3]^{2+}$ was studied by ^{17}O-NMR techniques, whereas the rate of anation according to (3) was used to derive estimates for the rate

$$[LM(bpy)(H_2O)]^{2+} + X \rightleftharpoons [LM(bpy)X]^{2+/+} + H_2O \quad (3)$$

constants of water exchange, k_{ex}, in $[Cp^*M(bpy)(H_2O)]^{2+}$ and $[L^{2-4}Ru(bpy)(H_2O)]^{2+}$ (X = Br^-, I^-, SCN^-, N_3^-, TU[7]).

Experimental Section

Unless stated otherwise, the metal salts, organic solvents, and ligands (reagent grade) were used without further purification. Silver perchlorate (Fluka) and silver sulfate (Merck) were carefully dried in vacuo. Silver tosylate and hexafluorophosphate were prepared from freshly precipitated silver carbonate and the appropriate acid. ^{17}O-enriched water (Yeda; 29.4 and 11.5 atom %) was used as received, whereas the normal deionized water was doubly distilled in a quartz apparatus before use.

The dinuclear complexes $[Cp^*MCl_2]_2$ (M = Co,[8a] Rh,[8b] Ir[8c]) and $[L^{2-4}RuCl_2]_2$,[8d,e] precursors for the preparation of the various complexes of the present study, were synthesized according to published procedures.

$[Cp^*Co(bpy)(H_2O)](PF_6)_2$.[8a] Samples of 100–200 mg of $[Cp^*CoCl_2]_2$ are hydrolyzed in 20–30 mL of water at ambient temperature. The stoichiometric amount of $AgPF_6$ is added, and the precipitating AgCl is removed by filtration. A slight excess of bpy is added to the filtrate, and after 15 min at 40 °C the reaction is completed, as indicated by a color change from blue to violet. Crystallization of the product is aided by the addition of a solution of $(NH_4)PF_6$ and cooling to 5 °C overnight (yield 50%; needle-shaped, small violet crystals). Anal. Calcd: C, 36.49; H, 3.83; N, 4.26. Found: C, 36.14; H, 3.75; N, 4.06.

$[Cp^*M(bpy)Cl]Cl$ (M = Rh,[8f] Ir[8g]) and $[L^{2-4}Ru(bpy)Cl]Cl$. A 100–150 mg sample of the corresponding dinuclear complex $[LMCl_2]_2$ is suspended in 30–40 mL of MeOH, and the stoichiometric amount of bpy is added at ambient temperature. After 10–15 min of stirring, the suspended material dissolves and a deep orange-red solution is obtained. After removal of most of the MeOH, small amounts of *n*-hexane are added to initiate the practically quantitative precipitation of the orange to red product complexes. They are isolated by filtration and washed with *n*-hexane.

Complexes $[Cp^*M(bpy)Cl]Cl$ (M = Rh, Ir] and $[LRu(bpy)Cl]Cl$ (L = L^2, L^3, L^4) gave satisfactory C,H,N analyses.

$[Cp^*Ir(OH_3)IrCp^*]OH\cdot 11H_2O$. A 150 mg of sample of $[Cp^*IrCl_2]_2$ is hydrolyzed in 45 mL of water at 70 °C to obtain a yellow solution of the cation $[Cp^*Ir(H_2O)_3]^{2+}$. The chloride ions are removed by addition of the stoichiometric amount of silver tosylate and filtration of the AgCl precipitated. The addition of 1 M NaOH to the filtrate and cooling to 5 °C overnight afford pale yellow needles of the dinuclear complex. Isolation by filtration and drying of these crystals leads to partial loss of crystal water and formation of a powder.

Solutions of $[Cp^*M(H_2O)_3]^{2+}$ (M = Rh, Ir) for ^{17}O-NMR Measurements. As described in the preceding paragraph, $[Cp^*MCl_2]_2$ is hydrolyzed in water at 70 °C and the solution is treated with stoichiometric amounts of silver tosylate, followed by filtration of precipitated AgCl. The compositions of the three solutions used for the NMR experiments are given in the caption to Figure 6.

Solutions of $[LM(bpy)(H_2O)]^{2+}$ (M = Co, Rh, Ir, Ru) for Kinetic Measurements. In the case of M = Co, the solutions are prepared by dissolving $[Cp^*Co(bpy)(H_2O)](PF_6)_2$ in water. For M = Rh, Ir, and Ru, about 150 mg of the corresponding chloro complex [LM(bpy)Cl]Cl is dissolved in about 50 mL of water, and the precipitation of AgCl is followed by potentiometric titration (Ag electrode) with a 0.01 M solution of silver perchlorate. After filtration of the AgCl, the filtrate is set to the desired concentration and ionic strength by diluting and addition of $NaClO_4$. The noncoordinating buffer 2,6-dimethylpyridine-3-sulfonic acid[9] (Merck) is used to adjust the pH to 4.8.

(2) (a) Merbach, A. E. *Pure Appl. Chem.* **1982**, *54*, 1479. (b) Merbach, A. E. *Pure Appl. Chem.* **1987**, *59*, 161. (c) Merbach, A. E.; Akitt, J. W. *NMR: Basic Princ. Prog.* **1990**, *24*, 189. (d) Lincoln, S. F.; Merbach, A. E. *Advances in Inorganic Chemistry*; Academic Press: London, 1994; in press.
(3) (a) Burgess, J. *Metal Ions in Solution*; Ellis Horwood: Chichester, U.K., 1978; p 335. (b) Wilkins, R. *Kinetics and Mechanism of Reactions of Transition Metal Complexes*; VCH Verlagsgesellschaft: Weinheim, Germany, 1991; p 214. (c) Crimp, S. J.; Spiccia, L.; Krouse, H. R.; Swaddle, T. W. *Inorg. Chem.* **1994**, *33*, 465.
(4) Rapaport, I.; Helm, L.; Merbach, A. E.; Bernhard, P.; Ludi, A. *Inorg. Chem.* **1988**, *27*, 873.
(5) Stebler-Röthlisberger, M.; Hummel, W.; Pittet, P. A.; Bürgi, H. B.; Ludi, A.; Merbach, A. E. *Inorg. Chem.* **1988**, *27*, 1358.
(6) Luginbühl, W.; Zbinden, P.; Pittet, P. A.; Armbruster, T.; Bürgi, H. B.; Merbach, A. E.; Ludi, A. *Inorg. Chem.* **1991**, *30*, 2350.
(7) Abbreviations used: L^1 = Cp* = η^5-pentamethylcyclopentadienyl anion; bpy = 2,2′-bipyridine; L^2 = C_6H_6 = η^6-benzene; L^3 = η^6-cymene = η^6-1-isopropyl-4-methylbenzene; L^4 = η^6-hexamethylbenzene; TU = thiourea; Me-im = *N*-methylimidazole.
(8) (a) Koelle, U.; Fuss, B. *Chem. Ber.* **1984**, *117*, 743, 753. (b) Kang, J. W.; Moseley, K.; Maitlis, P. M. *J. Am. Chem. Soc.* **1969**, *91*, 5970. Booth, B. L.; Hazeldine, R. N.; Hill, M. *J. Chem. Soc. A* **1969**, 1299. Kang, J. W.; Maitlis, P. M. *J. Chem. Soc. A* **1970**, 2875. (c) Bell, R. G.; Graham, W. A. G.; Heinekey, D. M. *Inorg. Chem.* **1990**, *29*, 2023. (d) Zelonka, R. A.; Baird, M. C. *Can. J. Chem.* **1972**, *50*, 3063. (e) Bennett, M. A.; Huang, T. N.; Matheson, T. W.; Smith, K. A. *Inorg. Synth.* **1982**, *21*, 74. (f) Koelle, U.; Grätzel, M. *Angew. Chem., Int. Ed. Engl.* **1987**, *26*, 567. (g) Ziessel, R. *Angew. Chem., Int. Ed. Engl.* **1991**, *30*, 844.
(9) Bips, U.; Elias, H.; Hauröder, M.; Kleinhans, G.; Pfeifer, S.; Wannowius, K. J. *Inorg. Chem.* **1983**, *22*, 3862.

Table 1. Crystallographic Data for [Cp*Rh(bpy)Cl]ClO_4, [Cp*Ir(bpy)Cl]ClO_4, and [Cp*Ir$(OH)_3$IrCp*]OH·11H_2O

	[Cp*Rh(bpy)Cl]ClO_4	[Cp*Ir(bpy)Cl]ClO_4	[Cp*Ir$(OH)_3$IrCp*]OH·11H_2O
chem formula	$C_{20}H_{23}Cl_2N_2O_4Rh$	$C_{20}H_{23}Cl_2IrN_2O_4$	$C_{20}H_{56}Ir_2O_{15}$
fw	529.23	618.54	921.09
space group	$Pmn2_1$ (No. 31)	$Pmn2_1$ (No. 31)	*Pnma* (No. 62)
a, Å	12.714(5)	12.714(4)	17.43(2)
b, Å	8.141(5)	8.216(4)	17.93(2)
c, Å	10.504(5)	10.507(4)	10.52(1)
V, Å^3	1087.73	1098.06	3304.9
Z	2	2	4
T, °C	26	23	19
ϱ(calcd), g cm^{-3}	1.62	1.87	1.86
μ, cm^{-1}	10.47	63.3	81.1
$R(F_o)$[a]	0.0378	0.0238	0.0359
$R_w(F_o)$[b]	0.0352	0.0235	0.0317

[a] $R(F_o) = \sum|F_o - F_c|/\sum F_o$. [b] $R_w(F_o) = \sum w^{1/2}|F_o - F_c|/\sum w|F_o|$.

Instrumentation: UV/vis spectra, diode array spectrophotometer (Hewlett-Packard, type 8451); pH measurements, micro glass electrode (Ingold, type U-402); anation kinetics, modified[10] stopped-flow spectrophotometer (Durrum, type D 110), ^{17}O-NMR, Bruker AM-400 spectrometer, equipped with 9.4-T wide-bore cryomagnet (54.25 MHz).

Spectrophotometric Titration. The equilibrium constants *K* for the anation reactions described by eq 3 were determined by spectrophotometric titration. The absorbance/[X] data for two different wavelengths were computer-fitted to eq 4 to obtain *K*.

$$A = (A_0 + A_\infty K[X])/(1 + K[X]) \quad (4)$$

The symbols A_0 and A_∞ refer to the absorbance of the species [LM(bpy)$(H_2O)]^{2+}$ and [LM(bpy)X]$^{2+}$, respectively, at the concentration of $[M]_{tot}$.

The acidity constants K_a for the deprotonation of the species [LM(bpy)$(H_2O)]^{2+}$ according to eq 5 were determined by spectrophotometric

$$[LM(bpy)(H_2O)]^{2+} \rightleftharpoons [LM(bpy)(OH)]^{+} + H^{+} \quad (5)$$

titration with NaOH. The *A*/*a* data (*a* = proton activity, as calculated from pH) were also computer-fitted to eq 4 with [X] = *a* and $K = 1/K_a$. A_0 and A_∞ refer to the absorbance of the species [LM(bpy)$(OH)]^+$ and [LM(bpy)$(H_2O)]^{2+}$, respectively, at the concentration of $[M]_{tot}$.

X-ray Structure Determination. The crystals of [Cp*Rh(bpy)Cl]ClO_4 (orange platelet, 0.06 × 0.21 × 1.2 mm^3) and [Cp*Ir(bpy)Cl]ClO_4 (yellow long platelet, 0.1 × 0.25 × 3.0 mm^3) chosen for X-ray measurements were grown from aqueous solutions of the corresponding chloro chlorides [Cp*M(bpy)Cl]Cl in the presence of an excess of $NaClO_4$ at ambient temperature. The crystal of [Cp*Ir$(OH)_3$IrCp*]OH·11H_2O (pale yellow flat prism, 0.25 × 0.50 × 0.60 mm^3) was grown from an aqueous solution upon cooling. It was transferred into the Lindemann capillary together with some mother liquor to avoid the loss of hydrate water. Intensities were measured on a four-circle diffractometer (Stoe-Stadi-4) using graphite-monochromatized Mo Kα radiation (λ = 0.710 69 Å; scan 2θ:ω = 1:1). Cell constants were determined by the least-squares method from the 2θ angles of 48 reflections for all complexes on the same instrument ([Cp*Rh(bpy)Cl]ClO_4, *T* = 299 K; [Cp*Ir(bpy)Cl]ClO_4, *T* = 296 K; [Cp*Ir$(OH)_3$IrCp*]OH·11H_2O, *T* = 292 K).

The structures were solved by direct methods with SHELXS-86 and refined by least-squares to the *R* values given in Table 1. Hydrogen atoms were positioned geometrically (C−H distance = 1.08 Å) and not refined. An empirical extinction correction was applied. All crystallographic calculations were performed with the programs SHELX-76 and SHELXS-86 on an IBM 3081 K computer at the Technische Hochschule Darmstadt. Scattering factors f_0, f', and f'' for C, H, N, and O are stored in SHELX-76.[11] The final positional parameters are given in Tables 2−4.

Table 2. Atomic Parameters (×10^4) for [Cp*Rh(bpy)Cl]ClO_4 (Excluding H and Perchlorate)

atom	*x*/*a*	*y*/*b*	*z*/*c*	U_{eq}, Å^2 [a]
Rh1	0	2352(1)	5000	383(2)
Cl1	0	5176(3)	5604(3)	561(7)
N1	1023(4)	3041(6)	3525(5)	435(14)
C1	582(4)	3630(7)	2422(6)	472(18)
C2	1173(5)	4202(8)	1460(6)	599(20)
C3	2259(5)	4159(9)	1529(7)	722(24)
C4	2719(5)	3536(9)	2622(7)	642(23)
C5	2078(5)	3013(8)	3585(7)	535(19)
C6	561(4)	−95(7)	5310(6)	532(21)
C7	893(5)	932(8)	6339(6)	547(20)
C8	0	1566(12)	6981(10)	620(32)
C9	1243(5)	−1054(8)	4408(7)	685(23)
C10	1989(6)	1175(12)	6800(9)	923(32)
C11	0	2618(15)	8140(11)	983(49)

[a] $U_{eq} = {}^1/_3(U_{11} + U_{22} + U_{33})$.

Table 3. Atomic Parameters (×10^4) for [Cp*Ir(bpy)Cl]ClO_4 (Excluding H and Perchlorate)

atom	*x*/*a*	*y*/*b*	*z*/*c*	U_{eq}, Å^2 [a]
Ir1	0	2351(1)	5000	398(1)
Cl1	0	5170(4)	5567(3)	576(8)
N1	1016(4)	3075(7)	3534(5)	429(16)
C1	588(5)	3645(9)	2449(6)	50(21)
C2	1193(6)	4235(10)	1476(7)	620(24)
C3	2261(6)	4195(11)	1562(7)	698(27)
C4	2712(6)	3561(11)	2648(7)	697(27)
C5	2079(5)	3007(10)	3622(7)	511(22)
C6	575(4)	−93(9)	5318(6)	491(22)
C7	912(5)	958(10)	6347(6)	519(22)
C8	0	1592(14)	6973(9)	600(34)
C9	1230(6)	−1047(11)	4432(7)	680(26)
C10	2008(6)	1176(13)	6842(9)	843(34)
C11	0	2681(18)	8180(13)	1004(60)

[a] $U_{eq} = {}^1/_3(U_{11} + U_{22} + U_{33})$.

NMR Measurements. The technical details[12] and the high-pressure probe[13] were described previously. ^{17}O-NMR chemical shifts are referred to water and measured with respect to ClO_4^- at 288 ppm.

The analysis of the experimental data using the appropriate equations was performed by a nonlinear least-squares program fitting the values of the desired parameters. Reported errors are 1 standard deviation.

Kinetic Measurements. The anation reactions according to eq 3 were followed by stopped-flow spectrophotometry in buffered aqueous solution (pH = 4.8; *I* = 0.3 M; *T* = 293 K) under pseudo-first-order conditions ($[complex]_0 \ll [X]_0$) at wavelengths in the range 350−650

(10) Elias, H.; Fröhn, U.; von Irmer, D.; Wannowius, K. J. *Inorg. Chem.* **1980**, *19*, 869.

(11) Data for Rh and Ir were taken from: *International Tables for X-ray Crystallography*; Kynoch Press: Birmingham, England, 1974; Vol. IV.

(12) Helm, L.; Elding, L. I.; Merbach, A. E. *Helv. Chim. Acta* **1984**, *67*, 1453.

(13) Frey, U.; Helm, L.; Merbach, A. E. *High Pressure Res.* **1990**, *2*, 237.

Table 4. Atomic Parameters (×10⁴) for [Cp*Ir(OH)₃IrCp*]OH·11H₂O (Excluding H)

atom	x/a	y/b	z/c	U_{eq}, Å² [a]
Ir1	1614(1)	2500	6938(1)	264(2)
Ir2	1932(1)	2500	4053(1)	265(2)
O1	2593(6)	2500	5746(8)	358(30)
O2	1342(4)	1806(3)	5351(6)	198(20)
C1	2122(9)	2500	8784(12)	419(49)
C2	2988(10)	2500	9016(16)	699(66)
C3	1681(7)	1849(6)	8630(9)	432(34)
C4	1926(8)	1044(6)	8744(11)	703(46)
C5	896(7)	2106(5)	8442(9)	425(34)
C6	189(8)	1594(7)	8249(12)	702(47)
C7	2822(9)	2500	2667(13)	423(49)
C8	3675(10)	2500	2983(16)	687(63)
C9	2346(7)	1853(5)	2505(9)	398(32)
C10	2617(9)	1034(6)	2534(12)	711(46)
C11	1578(6)	2090(5)	2232(9)	377(32)
C12	911(7)	1593(8)	1968(11)	739(48)
O3	3247(4)	967(3)	6008(6)	351(20)
O4	1715(5)	325(3)	5436(7)	542(25)
O5	4728(4)	1664(4)	148(6)	462(24)
O6	4564(5)	330(5)	1752(7)	702(30)
O7	3981(5)	470(4)	8391(8)	718(30)
O8	4462(6)	459(5)	4403(9)	976(40)

[a] $U_{eq} = {}^1/_3(U_{11} + U_{22} + U_{33})$.

nm. The *A*/*t* data, resulting from the observed decrease or increase in absorbance *A* with time *t*, were computer-fitted to eq 6 (irreversible first-order reaction). The program used was based on the least-squares method.

$$A = (A_0 - A_\infty)[\exp(-k_{obsd}t)] + A_\infty \quad (6)$$

Results

Preparation and Properties of the Complexes. As reviewed very recently,[14] the chloro-bridged dinuclear complexes $[LMCl_2]_2$ (M = Co(III), Rh(III), Ir(III), Ru(II)) are very useful precursors for the preparation of a variety of derivatives. Addition of 2,2′-bipyridine to $[LMCl_2]_2$, suspended in methanol, leads to the complexes [LM(bpy)Cl]Cl (L = L¹ = Cp* for M = Rh, Ir;[8f,g] L = L²–L⁴ for M = Ru), the hydrolysis of which affords the corresponding aqua species $[LM(bpy)(H_2O)]^{2+}$. Removal of the chloride ions from these solutions is easily achieved by precipitation of AgCl with silver perchlorate (see Experimental Section). Hydrolysis of $[LMCl_2]_2$ produces the triaqua cations $[LM(H_2O)_3]^{2+}$, which are remarkably stable in the case of M = Rh, Ir and L = Cp*. In acidic to neutral aqueous solution, the corresponding cobalt species $[Cp^*Co(H_2O)_3]^{2+}$ is of limited stability only ($t_{1/2}$ = 1–2 h). It can be stabilized, however, when two of the three water molecules are replaced by 2,2′-bipyridine to form the cation $[Cp^*Co(bpy)(H_2O)]^{2+}$, isolated as the hexafluorophosphate (see Experimental Section). The hydroxo-bridged dinuclear iridium species $[Cp^*Ir(OH)_3IrCp^*]^+$ is formed in alkaline solutions of $[Cp^*Ir(H_2O)_3]^{2+}$ and can be isolated as the hydroxide hydrate.

Table 5 summarizes the visible absorption data of the various arene aqua cations in aqueous solution. The increase in ligand field strength according to the spectrochemical series, as caused by the substitution of ligands such as thiocyanate and *N*-methylimidazole for water in $[LM(bpy)(H_2O)]^{2+}$, is clearly reflected by a blue shift of the absorption bands.

It follows from the pK_a values listed in Table 6 that the acidity of the coordinated water in the species $[Cp^*M(bpy)(H_2O)]^{2+}$ increases with decreasing charge density on the metal, though not much. The pK_a drops from 8.4 for M = Co to 8.2 for rhodium and 7.5 for iridium. This sort of metal effect, which makes $[Cp^*Ir(bpy)(H_2O)]^{2+}$ the most acidic species, is opposite to that expected on simple electrostatic grounds and testifies to the increasing covalency of the metal–water bond down the triad. The effect of the variation of the arene ligand L in $[LRu(bpy)(H_2O)]^{2+}$ on the pK_a is very small indeed. The pK_a changes from 6.9 (L²) to 7.2 (L³) and 7.3 (L⁴). Hexamethylbenzene (L⁴) and cymene (L³) make the coordinated water slightly less acidic than benzene (L²), which is in line with the stronger donor character of these alkylated arene ligands. It is important to note that, for all of the aqua cations listed in Table 6, the pK_a is such that the fraction of the hydroxo species $[LM(bpy)(OH)]^+$ is negligibly small at the pH of the kinetic studies.

Structures. Complexes $[Cp^*Rh(bpy)Cl]ClO_4$ and $[Cp^*Ir(bpy)Cl]ClO_4$ crystallize in the orthorhombic space group $Pmn2_1$ and are isostructural. Figure 1 gives a view of the coordination geometry in the cation $[Cp^*Rh(bpy)Cl]^+$ which demonstrates that the atoms Rh, Cl, C8, and C11 lie on a mirror plane which cuts the complex unit into identical halves. The same highly symmetric arrangement is found for the cation $[Cp^*Ir(bpy)Cl]^+$. The view along the *a* axis of the unit cell (Figure 2) shows that both the ligands Cp* and bpy as such are practically planar and that the perchlorate ions are not coordinated.

Table 7 summarizes some relevant angles and distances, which reflect the close structural similarity between $[Cp^*Rh(bpy)Cl]ClO_4$ and $[Cp^*Ir(bpy)Cl]ClO_4$, which was also reported for the Rh/Ir couple $[Cp^*RhCl_2]_2$ and $[Cp^*IrCl_2]_2$.[15]

Table 5. Visible Absorption [λ_{max}, nm (ϵ_{max}, M^{-1} cm^{-1})] of the Complex Cations[a] in Aqueous Solution[b]

	M		
	Co	Rh	Ir
$[Cp^*M(bpy)(H_2O)]^{2+}$	530 (750)	358 (2550)	(3000)[c]
$[Cp^*M(bpy)(SCN)]^+$	525 (995)	(4000 at 360 nm)	(4000)[c]
$[Cp^*M(bpy)I]^+$	560 (910)	400 sh (3400)	380 sh (4200)
$[Cp^*M(bpy)Br]^+$	545 (845)	378 (2730)	370 sh (4200)
$[Cp^*M(bpy)(TU)]^{2+}$	532 (1190)	360 sh (3900)	(4100)[c]
$[Cp^*M(bpy)(Me\text{-}im)]^{2+}$	510 (900)		
$[Cp^*M(bpy)N_3]^+$		(3200 at 360 nm)	(4000)[c]
$[Cp^*M(H_2O)_3]^{2+}$	600 (580)	375 (1640)	(3000)[c]

	X					
	H_2O	SCN^-	I^-	Br^-	TU	Me-im[d]
$[L^2Ru(bpy)X]^{2+/+}$	(3150)[c]	*e*	*e*	*e*	*e*	*e*
$[L^3Ru(bpy)X]^{2+/+}$	(3140)[c]	(4860)[c]	(4780)[c]	(4120)[c]	(4970)[c]	(3970)[c]
$[L^4Ru(bpy)X]^{2+/+}$	(3200)[c]	*e*	*e*	*e*	*e*	*e*

[a] The spectral data were obtained from solutions of $[LM(bpy)(H_2O)]^{2+}$ which were reacted with an excess of the corresponding monodentate ligand X. [b] At pH = 4.8, 293 K, and I = 0.3 M ($NaClO_4$). [c] Flat spectrum without absorption maximum; the absorptivity listed refers to 380 nm. [d] Me-im = *N*-methylimidazole. [e] The absorptivities of $[L^2Ru(bpy)X]^{2+}$ and $[L^4Ru(bpy)X]^{2+}$ are very close to those of $[L^3Ru(bpy)X]^{2+}$.

Table 6. Acidity Constants pK_a of the Monoaqua Arene Species $[LM(bpy)(H_2O)]^{2+}$ and Equilibrium Constants for the Anation According to (3) at 298 K[a]

	M		
	Co	Rh	Ir
$[Cp^*M(bpy)(H_2O)]^{2+}$	8.4 ± 0.15 30.5 ± 4.5[b] 79.1 ± 8.0[c]	8.2 ± 0.15 1850 ± 150[b]	7.5 ± 0.15

	L		
	L^2	L^3	L^4
$[LRu(bpy)(H_2O)]^{2+}$	6.9 ± 0.1	7.2 ± 0.1	7.3 ± 0.1

[a] I = 0.5 M ($NaClO_4$). [b] Equilibrium constant K (M^{-1}) for the anation reaction with X = Br^- according to eq 3. [c] K for the anation according to eq 3 with X = Me-im.[7]

(14) Koelle, U. *Coord. Chem. Rev.*, in press.

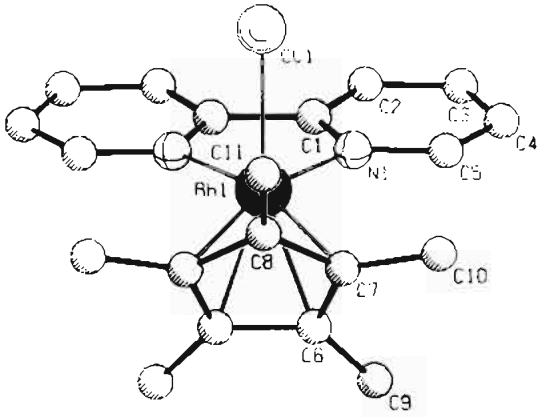

Figure 1. View of the coordination geometry in the complex cation $[Cp^*Rh(bpy)Cl]^+$.

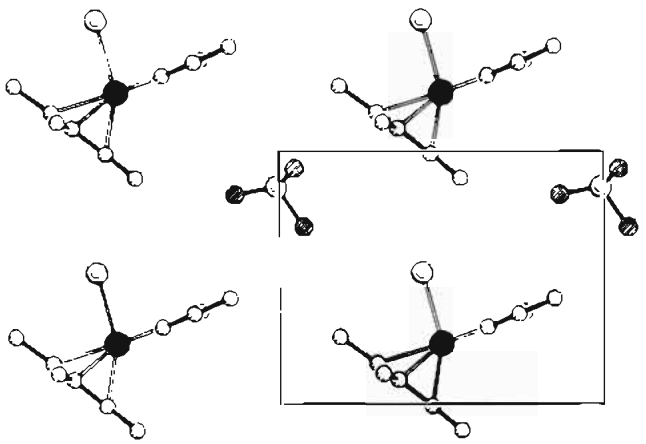

Figure 2. Projection of the unit cell of the complex $[Cp^*Rh(bpy)Cl]ClO_4$ along the *a* axis.

Table 7. Selected Distances (Å) and Bond Angles (deg) for $[Cp^*Rh(bpy)Cl]ClO_4$ and $[Cp^*Ir(bpy)Cl]ClO_4$

	Distances	
	M = Rh	M = Ir
M−Cl	2.385(2)	2.391(3)
M−N	2.100(5) (2×)	2.097(5) (2×)
M−C	2.141(6) (2×)	2.160(6) (2×)
	2.146(6) (2×)	2.162(7) (2×)
	2.178(10) (1×)	2.167(10) (1×)
	2.151[a]	2.162[a]
M−Cp*[b]	1.776	1.781
	Angles	
	M = Rh	M = Ir
N−M−N	76.6(3)	76.1(3)
N−M−Cl	86.5(1)	84.8(2)
P1−P2[c]	0.38	0.55
P1−P3[c]	61.05	62.47

[a] Average distance. [b] Distance between M and the center of the Cp* ring. [c] P1 = plane of the first pyridine ring in the ligand bpy; P2 = plane of the second pyridine ring in the ligand bpy; P3 = plane of the Cp* ring, as formed by the five C atoms forming the ring.

The dinuclear, triply hydroxo-bridged iridium complex $[Cp^*Ir(OH)_3IrCp^*]OH\cdot 11H_2O$ crystallizes in the orthorhombic space group *Pnma* and is also isostructural with the corresponding rhodium complex.[16] As shown in Figure 3, the three coordinated hydroxyl groups lie on a mirror plane with the plane

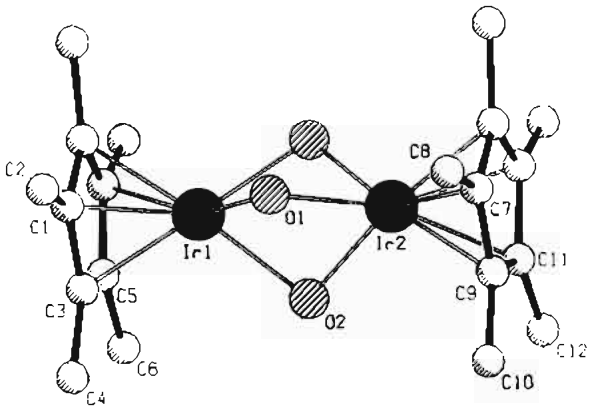

Figure 3. View of the coordination geometry in the complex cation $[Cp^*Ir(OH)_3IrCp^*]^+$.

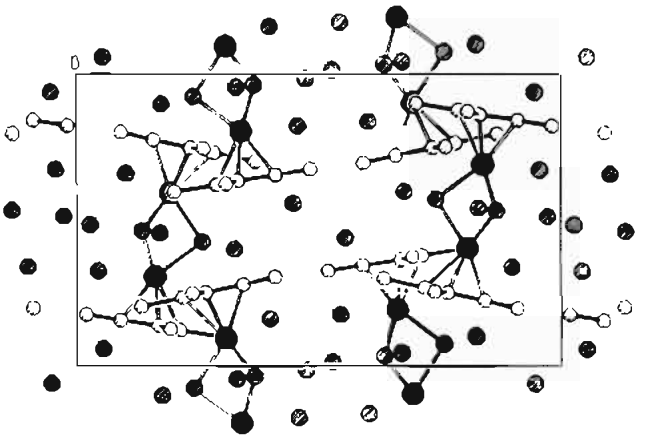

Figure 4. Projection of the unit cell of the complex $[Cp^*Ir(OH)_3IrCp^*]OH\cdot 11H_2O$ along the *b* axis. The isolated hatched circles represent water molecules and/or hydroxyl ions.

of the two Cp* ligands located practically parallel to it. Figure 4 indicates that the dinuclear complex cations are embedded in a hydrogen-bonded network of water molecules and the one hydroxyl ion per cation. In this network of water molecules, which stabilizes the structure,[17] the protons have a high mobility so that the hydroxyl counterion, neutralizing the monovalent complex cation, cannot be located crystallographically. Relevant distances and angles, as compiled in Table 8, document the structural similarity between $[Cp^*Ir(OH)_3IrCp^*]OH\cdot 11H_2O$ and the corresponding rhodium complex, analyzed by Nutton et al.[16]

Kinetics of Anation. One would expect that the coordinated water molecule in the species $[LM(bpy)(H_2O)]^{2+}$ is easily replaced when stronger nucleophiles are offered. To confirm this, the anation of $[Cp^*Co(bpy)(H_2O)]^{2+}$ by bromide ions and *N*-methylimidazole and of $[Cp^*Rh(bpy)(H_2O)]^{2+}$ by bromide ions was studied spectrophotometrically. The corresponding equilibrium constants *K* are 30.5, 79.1, and 1850 M^{-1}, respectively (see Table 6).

The anation of the complexes $[LM(bpy)(H_2O)]^{2+}$ according to eq 3 was studied at pH 4.8 by stopped-flow spectrophotometry under pseudo-first-order conditions. The change in absorbance with time could be well fitted to the exponential (6), which means that the rate of anation is first-order in complex. As an example, Figure 5 shows the plot of the experimental rate constant, k_{obsd}, versus the excess concentration of the entering ligand X for three different systems. The dependencies $k_{obsd} = f([X])$ are in all cases straight lines without intercept, which

(15) (a) Churchill, M. R.; Julius, S. A.; Rotella, F. J. *Inorg. Chem.* **1977**, *16*, 1137. (b) Churchill, M. R.; Julis, S. A. *Inorg. Chem.* **1977**, *16*, 1488.

(16) Nutton, A.; Baily, P. M.; Maitlis, P. M. *J. Chem. Soc., Dalton Trans.* **1981**, 1997.

(17) Drying of $[Cp^*Ir(OH)_3IrCp^*]OH\cdot 11H_2O$ over P_2O_5 leads to a dark-brown powder. Addition of water regenerates pale-yellow crystals of $[Cp^*Ir(OH)_3IrCp^*]OH\cdot 11H_2O$.

Table 8. Selected Distances (Å) and Bond Angles (deg) for $[Cp^*Ir(OH)_3IrCp^*]OH\cdot 11H_2O$ and $[Cp^*Rh(OH)_3RhCp^*]OH\cdot 11H_2O$

Distances

	M = Ir	M = Rh[16]
M1−O	2.135(6) (2×)	2.106(3) (2×)
	2.118(9) (1×)	2.112(4) (1×)
M2−O	2.115(6) (2×)	2.104(3) (2×)
	2.122(9) (1×)	2.124(4) (1)
	2.123(3)[a]	2.110(4)[a]
M1−C[b]	2.134	2.127
M2−C[b]	2.134	2.129
M−Cp*[c]	1.750	
M1−M2	3.086(1)	2.974(1)

Angles

	M = Ir	M = Rh[16]
O−M1−O	71.3(1) (1×)	76.5(1) (2×)
	73.5(1) (2×)	74.6(1) (1×)
O−M2−O	73.8(3) (2×)	76.2(1) (2×)
	72.1(1) (1×)	74.7(1) (1×)
	73.0(2)[a]	75.8(1)[a]
M1−O−M2	93.4(2) (1×)	89.2(1) (1×)
	93.1(1) (2×)	89.9(1) (2×)
O−O−O	60.7 (2×)	60.7(1) (2×)
	58.6 (1×)	58.6(1) (1×)

[a] Average value. [b] Averaged distance between M and the C atoms forming the Cp* ring. [c] Distance between M and the center of the Cp* ring.

corresponds to rate law 7 with second-order rate constant k_X

$$d[LM(bpy)X^+]/dt = k_{obsd}[LM(bpy)(H_2O)^{2+}] = k_X[X][LM(bpy)(H_2O)^{2+}] \quad (7)$$

resulting from the slope of the plots of k_{obsd} vs [X]. It follows from the summary of rate constants k_X in Table 10 that (i) for a given entering ligand X the order of reactivity is Rh > Ir ≫ Co and (ii) for a given complex the neutral ligands X react more slowly than the anionic ones.

According to the Eigen−Wilkins mechanism, the anation of an aqua cation M is a two-step process with outer-sphere complex formation (eq 8) preceding ligand interchange (eq 9).

$$M + X \xrightarrow{K_{os}} \{M,X\} \quad (8)$$

$$\{M,X\} \xrightarrow{k_i} M-X \quad (9)$$

For [M] ≪ [X], the experimental rate constant k_{obsd} should obey relationship 10, which is reduced to the simple dependence (11)

$$k_{obsd} = (k_i K_{os}[X])/(1 + K_{os}[X]) \quad (10)$$

$$k_{obsd} = k_i K_{os}[X] \quad (11)$$

for $K_{os}[X] \ll 1$. This latter condition is obviously fulfilled for the present systems, so that the experimentally determined second-order rate constant k_X corresponds to the product $k_i K_{os}$. Since K_{os} can be calculated on the basis of the Fuoss−Eigen electrostatic model,[18] the rate constant for the interchange step (9), k_i, becomes available (see Table 9). One recognizes that, for a given complex $[LM(bpy)(H_2O)]^{2+}$, the data for k_i thus obtained are of similar size, independent of the charge and nature of X.

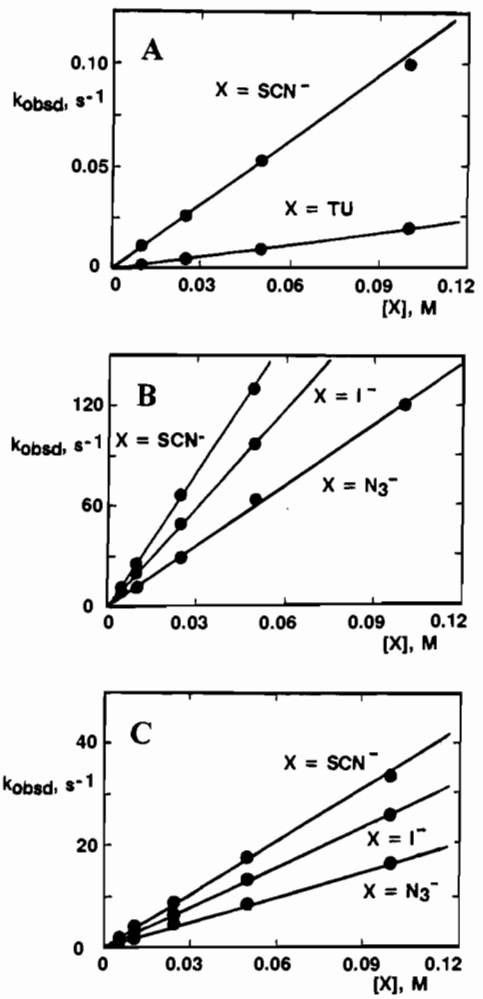

Figure 5. Plots of the experimental rate constant k_{obsd} vs [X] for the reaction of $[Cp^*M(bpy)(H_2O)]^+$ (M = Co (A), Rh (B), Ir (C)) with various nucleophiles X at 293 K according to (3).

Table 10 presents the activation parameters for the anation of the various complexes with TU and thiocyanate or bromide ion. The parameters determined from the temperature dependence of rate constant k_X are of limited value only, since k_X is a composite parameter ($k_X = k_i K_{os}$). For the neutral ligand X = Tu, however, the data for $\Delta H^{\ddagger}$ and $\Delta S^{\ddagger}$ were obtained from the temperature dependence of $k_i = k_X/K_{os}$ (for neutral ligands, $K_{os} \neq f(T)$[18]). The entropy of activation, obtained with rather high limits of error, is either negative or close to zero.

NMR Measurements: Water Exchange. The measured ^{17}O-NMR spectra display two resonances due to ClO_4^- at 288 ppm and to the three bound water molecules in $[Cp^*M(H_2O)_3]^{2+}$ at −64 ppm for M = Rh or −60 ppm for M = Ir. $Mn(ClO_4)_2$ was added to the solutions as a relaxation agent to allow accurate measurements of the line width of the bound-water signal. The numbers of coordinated water molecules, as obtained by NMR integrals with $[Be(H_2O)_4]^{2+}$ as internal standard, are 2.7 ± 0.3 and 2.8 ± 0.3 for Rh and Ir, respectively.

In the limit of slow exchange,[19] the bound water−^{17}O relaxation rate is given by eq 12, where τ is the mean lifetime

$$1/T_2^b = 1/\tau + 1/T_{2Q}^b \quad (12)$$

of water in the first coordination sphere and $1/T_{2Q}^b$ is the quadrupolar relaxation rate.

(18) As outlined in detail in ref 3b (pp 206−207), the calculation is based on the equation $K_{os} = \alpha \exp(-U/kT)$, with $\alpha = (4\pi Na^3)/3000$ (a = distance of closest approach of the reacting ions) and the Debye−Hückel interionic potential U, which depends on the charge z of the reactants, the ionic strength and dielectric constant of the medium, and the parameter a. It should be noted that $\alpha \neq f(T)$ and $U = 0$ for neutral ligands X.

(19) McLaughlin, A. C.; Leigh, J. S. *J. Magn. Reson.* **1973**, *9*, 296.

Table 9. Rate Constants k_X (M^{-1} s^{-1})[a] and k_i (s^{-1}) for the Anation of Complexes $[LM(bpy)(H_2O)]^{2+}$ with Ligands X According to (3) at 293 K (pH 4.8; I = 0.3 M)

	X					
	SCN^-	I^-	Br^-	N_3^-	TU	Me-im
	$[Cp^*Co(bpy)(H_2O)]^{2+}$ (k_i(average) = 0.60 ± 0.29[b])					
k_X	1.050 ± 0.050[c]	0.780 ± 0.040	0.439 ± 0.030		0.192 ± 0.010[c]	0.055 ± 0.005
k_i[d]	0.875	0.650	0.366		0.873	0.250
	$[Cp^*Rh(bpy)(H_2O)]^{2+}$ (k_i(average) = 1590 ± 760[b])					
k_X	2750 ± 250	2060 ± 200	640 ± 40	1190 ± 80	460 ± 25	
k_i[e]	2500	1870	580	1080	1920	
	$[Cp^*Ir(bpy)(H_2O)]^{2+}$ (k_i(average) = 219 ± 85[b])					
k_X	342 ± 20	285 ± 15	110 ± 6	181 ± 9	62 ± 4	
k_i[e]	310	260	100	164	260	
	$[L^2Ru(bpy)(H_2O)]^{2+}$ (k_i(average) = 0.0680 ± 0.038[b])					
k_X	0.115 ± 0.020	0.060 ± 0.020	0.041 ± 0.010		0.027 ± 0.007	0.008 ± 0.002
k_i[e]	0.104	0.054	0.037		0.113	0.033
	$[L^3Ru(bpy)(H_2O)]^{2+}$ (k_i(average) = 0.085 ± 0.048[b])					
k_X	0.141 ± 0.020	0.073 ± 0.015	0.045 ± 0.010		0.035 ± 0.005	0.011 ± 0.003
k_i[e]	0.128	0.066	0.041		0.146	0.046
	$[L^4Ru(bpy)(H_2O)]^{2+}$ (k_i(average) = 0.102 ± 0.054[b])					
k_X	0.151 ± 0.020	0.077 ± 0.020	0.048 ± 0.006		0.038 ± 0.005	
k_i[e]	0.137	0.070	0.043		0.158	

[a] Obtained from the slope of the plot of k_{obsd} vs [X] according to rate law 7, with k_{obsd} determined at five different concentrations of X in the range [X] = 0.005−0.1 M and [complex]$_0$ = (1−6) × 10^{-4} M. [b] As obtained by averaging all of the k_i values determined. [c] These data were taken from an earlier publication: Schneider, J. St.; Elias, H.; Kölle, U. *J. Serb. Chem. Soc.* **1990**, *55*, 695. [d] As calculated from $k_i = k_X/K_{os}$ with K_{os} = 1.20 M^{-1} for charged ligands X^- and K_{os} = 0.22 M^{-1} for neutral ligands X with a = 4.5 Å.[18] [e] As calculated from $k_i = k_X/K_{os}$ with K_{os} = 1.10 M^{-1} for charged ligands X^- and K_{os} = 0.24 M^{-1} for neutral ligands X with a = 4.6 Å.[18]

Table 10. Activation Parameters[a] for the Anation of Complexes $[LM(bpy)(H_2O)]^{2+}$ According to (3)

complex	X	$\Delta H^{\ddagger}$, kJ mol^{-1}	$\Delta S^{\ddagger}$, J mol^{-1} K^{-1}
$[Cp^*Co(bpy)(H_2O)]^{2+}$	SCN^-	75.9 ± 3.0	13 ± 5
	Br^-	74.4 ± 4.0	2 ± 8
	TU[b]	70.5 ± 4.0	−6 ± 7
$[Cp^*Rh(bpy)(H_2O)]^{2+}$	Br^-	49.2 ± 3.0	−22 ± 10
	TU[b]	47.9 ± 3.0	−18 ± 9
$[Cp^*Ir(bpy)(H_2O)]^{2+}$	Br^-	60.9 ± 3.0	2 ± 8
	TU[b]	59.1 ± 5.0	4 ± 9
$[L^2Ru(bpy)(H_2O)]^{2+}$	SCN^-	70.5 ± 3.5	−22 ± 8
	TU[b]	67.5 ± 3.8	−31 ± 9
$[L^3Ru(bpy)(H_2O)]^{2+}$	SCN^-	70.1 ± 3.0	−22 ± 7
	TU[b]	66.4 ± 2.8	−33 ± 8
$[L^4Ru(bpy)(H_2O)]^{2+}$	SCN^-	69.8 ± 3.6	−22 ± 7
	TU[b]	65.7 ± 3.6	−34 ± 8

[a] From the temperature dependence of k_X at four to eight temperatures in the range 287−319 K. [b] Activation parameters obtained from the temperature dependence of $k_i = k_X/K_{os}$ at four to eight temperatures in the range 287−319 K.

NMR Measurements: Variable Temperature. The temperature dependence of $1/\tau$ and its relaxation to the pseudo-first-order rate constant, k, for the exchange of a particular water molecule[20] can be expressed by the Eyring equation.[21] The quadrupolar relaxation rate ($1/T_{2Q}^b$) was assumed to obey an Arrhenius temperature dependence.[12]

It is evident from the results shown in Figure 6 that the observed relaxation rate $1/T_2^b$ is mainly governed, in the temperature range studied, by the kinetic contribution, in both $[Cp^*M(H_2O)_3]^{2+}$ (Rh, Ir) complexes. Therefore, it was not possible to adjust independently E_Q^b and $(1/T_{2Q}^b)^{298}$.[8] To be able to fit the data, the parameter E_Q^b had to be fixed. The known activation energies for the ^{17}O quadrupolar relaxation rate on water coordinated to a diamagnetic metal center range from 16.6 to 24.0 kJ mol^{-1}.[22] The different values for E_Q, fixed at 15, 20, and 25 kJ mol^{-1} during the fitting procedure, did not affect the results of the kinetic parameters (k^{298}, $\Delta H^{\ddagger}$, and $\Delta S^{\ddagger}$) within statistical error. All data obtained for the rhodium and iridium complexes are presented in Figure 6 and Table SXIII (supplementary material). The values of $(1/T_{2Q}^b)^{298}$, $\Delta H^{\ddagger}$, $\Delta S^{\ddagger}$, and k^{298} for $[Cp^*M(H_2O)_3]^{2+}$ (Rh, Ir) are reported in Table 11.

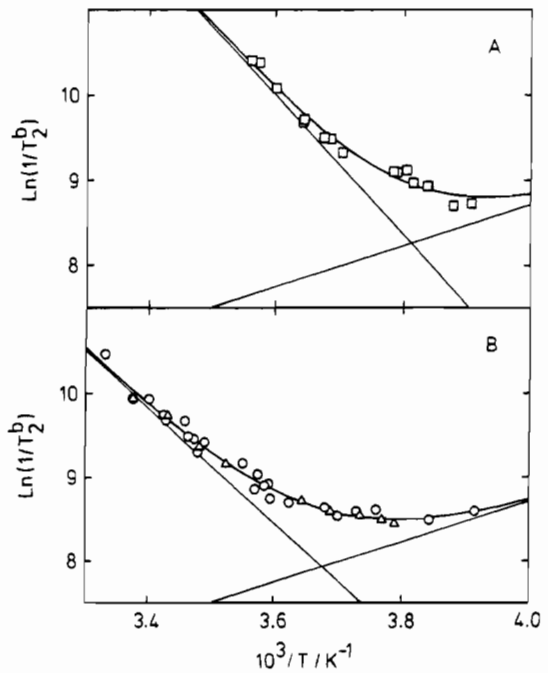

Figure 6. Temperature dependence of the relaxation rates, $1/T_2^b$, for the bound-water ^{17}O NMR signal of $[Cp^*M(H_2O)_3](tos)_2$ (M = Rh (A), Ir (B)) with the following compositions [solution, M, $[Cp^*M(H_2O)_3](tos)_2$] (*m*), $[HClO_4]$ (*m*), $[Mn(ClO_4)_2]$ (*m*), atom % of $H_2{}^{17}O$]: (□) 1, Rh, 0.088, 0.111, 0.820, 14.7; (○) 2, Ir, 0.163, 0.097, 0.392, 14.7; (△) 3, Ir, 0.190, 0.095, 0.411, 4.26.

NMR Measurements: Variable Pressure. The pressure dependence of the exchange rate can be described by the linear

(20) Swaddle, T. W. In *Advances in Inorganic and Bioinorganic Mechanisms*; Sykes, A. G., Ed.; Academic: London, 1983; Vol. 2, p 121.
(21) Eyring, H. *J. Chem. Phys.* **1935**, *3*, 107.
(22) For example: $[M(\eta^6\text{-}C_6H_6)(H_2O)_3]^{2+}$ E_Q^b = 23.7 kJ mol^{-1} [23] (M = Ru), E_Q^b = 24.0 kJ mol^{-1} [5] (M = Os), $[Pd(Me_5dien)H_2O]^{2+}$ E_Q^b = 16.6 kJ mol^{-1},[24] and $[Pd(Et_5dien)H_2O]^{2+}$ E_Q^b = 18.1 kJ mol^{-1}.[23]
(23) Berger, J.; Kotowski, M.; van Eldik, R.; Frey, U.; Helm, L.; Merbach, A. E. *Inorg. Chem.* **1989**, *28*, 3759.

Table 11. Kinetic and NMR Parameters Obtained from Variable-Temperature ^{17}O-NMR of Bound-Water Transverse Relaxation Rates of $[Cp^*M(H_2O)_3]^{2+}$ (M = Rh, Ir)

	$[Cp^*Rh(H_2O)_3]^{2+}$	$[Cp^*Ir(H_2O)_3]^{2+}$
$10^{-4}k^{298}$, s^{-1}	16 ± 3 (17.5, 15.0)	2.53 ± 0.08 (2.51, 2.53)
$\Delta H^{\ddagger}$ kJ mol^{-1}	65.6 ± 7 (69.3, 62.6)	54.9 ± 3 (58.2, 52.2)
$\Delta S^{\ddagger}$, JK^{-1} mol^{-1}	+75.3 ± 24 (+88.1, 64.6)	+23.6 ± 8 (+34.4, +14.4)
$(1/T_{2Q}^{b})^{298}$, s^{-1}	1294 ± 197 (1900, 880)	1282 ± 76 (1770, 925)
E_Q^b, kJ mol^{-1} [a]	20 (15, 25)	20 (15, 25)

[a] The value of the activation energy E_Q^b was fixed during the fitting procedure.

equation (13), since one can assume that the corresponding

$$\ln(k) = \ln((k)_0) - P\Delta V^{\ddagger}/RT \qquad (13)$$

volumes of activation are pressure independent, as is usual for simple solvent-exchange reactions.[24] $(k)_0$ is the exchange rate constant at zero pressure, and $\Delta V^{\ddagger}$ is the activation volume.

A similar equation, eq 14, describes the pressure dependence of the quadrupolar relaxation rate as a function of the quadrupolar activation volume, $\Delta V_Q^{\ddagger}$, and the contribution at zero pressure, $(1/T_{2Q}^{b})_0$.

$$\ln(1/T_{2Q}^{b}) = \ln((1/T_{2Q}^{b})_0) - P\Delta V_Q^{\ddagger}/RT \qquad (14)$$

For each complex, two series of variable-pressure experiments were performed at two temperatures and the data adjusted simultaneously to eqs 12−14. This requires us in principle to adjust six parameters, $\Delta V^{\ddagger}$ and $\Delta V_Q^{\ddagger}$, as well as $\ln((k)_0)$ and $\ln((1/T_{2Q}^{b})_0)$ at both temperatures, which is too much with the data sets available. To reduce the number of adjustable parameters to 4, as a constrain (eq 15) the percentage p of the quadrupolar $(1/T_{2Q}^{b})_0$ contribution to $(1/T_{2Q}^{b})_0$ was added, which can be calculated at both temperatures from the variable-temperature studies (see Table SXIV, supplementary material).

$$(1/T_{2Q}^{b})_0 = p(1/T_2^{b})_0 \qquad (15)$$

In the case of $[Cp^*Rh(H_2O)_3]^{2+}$, it was not possible to choose a temperature where the pressure dependence of the quadrupolar relaxation rate is properly defined. It was therefore necessary to fix also $\Delta V_Q^{\ddagger}$. The known $\Delta V_Q^{\ddagger}$ values for water bound in different complexes are small and within $\Delta V_Q^{\ddagger} \pm 1$ cm^3 mol^{-1}.[25]

It is reasonable to assume that the pressure dependence of $1/T_{2Q}^{b}$ for bound water molecules in $[Cp^*Rh(H_2O)_3]^{2+}$ is similar to that obtained for $[Cp^*Ir(H_2O)_3]^{2+}$. Therefore, the quadrupolar activation volume was fixed at $+0.5 \pm 1$ cm^3 mol^{-1}. The different values of $\Delta V_Q^{\ddagger}$, fixed during the fitting procedure, did not change significantly the value of the kinetic activation volume, within the statistical error. The values of $1/T_2^{b}$ as a function of pressure are presented in Figure 7 and Table SXV (supplementary material), and the results are given in Table 12.

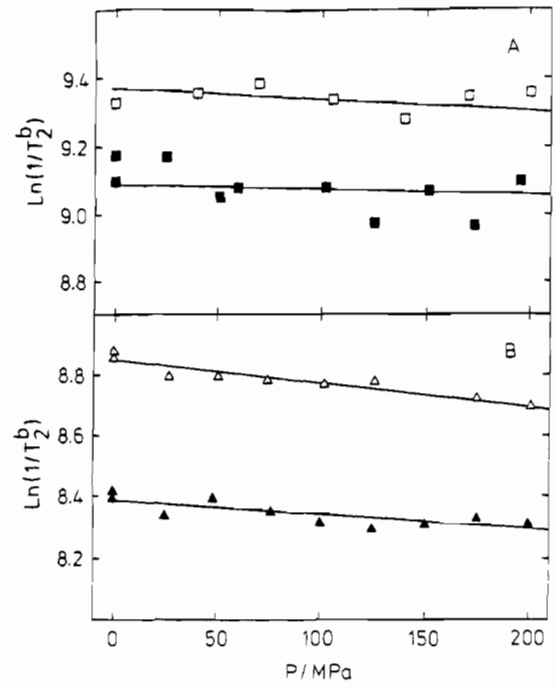

Figure 7. Pressure dependence of the transverse relaxation rates, $1/T_2^{b}$, for $[Cp^*M(H_2O)_3](tos)_2$ aqueous solutions (see Figure 6 for the composition): (A) M = Rh, solution 1, (■) at T = 264.3 K and (□) at T = 271 K; (B) M = Ir, solution 3, (▲) at T = 266.7 K and (△) at T = 281 K.

Discussion

The present study is focused on the substitution lability of the water coordinated in the half-sandwich monoaqua cations $[LM(bpy)(H_2O)]^{2+}$ (M = Co, Rh, Ir, Ru) and half-sandwich triaqua cations $[Cp^*M(H_2O)_3]^{2+}$ (M = Rh, Ir), which is governed by the steric and electronic effects caused by the metal M and its ligand field.

The results of the X-ray structure analysis document that the coordination geometries of the species $[Cp^*Rh(bpy)Cl]^{2+}$ and $[Cp^*IrM(bpy)Cl]^{2+}$ are practically identical (see Figure 1 and Table 7). It is very reasonable to assume that this holds for the corresponding aqua complexes $[Cp^*M(bpy)(H_2O)]^{2+}$ (M = Rh, Ir) as well and also for the homologous cobalt complex $[Cp^*Co(bpy)(H_2O)]^{2+}$ and the ruthenium complexes $[L^{2-4}Ru(bpy)(H_2O)]^{2+}$. From the steric point of view, the water position in $[LM(bpy)(H_2O)]^{2+}$ (M = Co, Rh, Ir, Ru) should thus be easily accessible and, more important, embedded in the same ligand geometry. On the basis of the close structural similarity between $[Cp^*Ir(OH)_3IrCp^*]OH{\cdot}11H_2O$ and $[Cp^*Rh(OH)_3RhCp^*]OH{\cdot}11H_2O$ (see Figure 3 and Table 8), one can conclude that the coordination geometries in the kinetically studied triaqua species $[Cp^*Rh(H_2O)_3]^{2+}$ and $[Cp^*Ir(H_2O)_3]^{2+}$ are also very similar.

The acidity of the coordinated water molecule in the species $[LM(bpy)(H_2O)]^{2+}$ can be taken as an indirect measure for the M−O bond strength and formal charge on the metal, respectively. It follows from Table 6 that the metal effect on the pK_a of the coordinated water in $[Cp^*M(bpy)(H_2O)]^{2+}$ (M = Co, Rh, Ir) is very minor indeed. Although the effective ionic radius of the six-coordinate low-spin Co^{3+} ion is smaller ($r(Co^{3+})$: $r(Rh^{3+})$:$r(Ir^{3+})$ = 68.5:80.5:82 pm), there is practically no difference in the pK_a values between the cobalt and rhodium complexes and only the iridium complex is by about $^1/_2$ pK_a unit more acidic. The variation in L affects the pK_a of the water in $[L^{2-4}Ru(bpy)(H_2O)]^{2+}$ very little. It should be noted however that the water is by about 1 pK_a unit more acidic in these complexes than in $[Cp^*M(bpy)(H_2O)]^{2+}$ (M = Co, Rh, Ir), which would predict a somewhat reduced mobility of the water in $[L^{2-4}Ru(bpy)(H_2O)]^{2+}$ compared to $[Cp^*M(bpy)(H_2O)]^{2+}$.

Considering the anation kinetics of the species $[Cp^*M(bpy)(H_2O)]^{2+}$ (M = Co, Rh, Ir) and $[L^{2-4}Ru(bpy)(H_2O)]^{2+}$, one is dealing with two series of complexes, which have the same overall charges and practically the same coordination geometries. Moreover, the M−O bond strength, as indirectly characterized by the $pK_a(H_2O)$ values, appears to be very similar. The rate

(24) Ducommun, Y.; Newmann, K. E.; Merbach, A. E. *Inorg. Chem.* **1980**, *19*, 3696.

(25) $[Pd(Me_5dien)H_2O]^{2+}$ $\Delta V_Q^{\ddagger} = -0.8$ cm^3 mol^{-1},[24] $[Pd(Et_5dien)H_2O]^{2+}$ $\Delta V_Q^{\ddagger} = -1$ cm^3 mol^{-1},[24] and $[Os(\eta^6\text{-}C_6H_6)(H_2O)_3]^{2+}$ $\Delta V_Q^{\ddagger} = -1$ cm^3 mol^{-1}.[23]

Table 12. Activation Volumes from Variable-Pressure ^{17}O-NMR Bound-Water Transverse Relaxation Rates of $[Cp^*M(H_2O)_3]^{2+}$

	$[Cp^*Rh(H_2O)_3]^{2+}$	$[Cp^*Ir(H_2O)_3]^{2+}$
$\Delta V^{\ddagger}$, cm^3 mol^{-1}	$+0.6 \pm 0.6$ ($+1.1$, $+0.2$)	$\Delta V^{\ddagger}$, cm^3 mol^{-1} $+2.4 \pm 0.5$
$\Delta V_Q^{\ddagger}$, cm^3 mol^{-1} [a]	$+0.5$ (-0.5, $+1.5$)	$\Delta V_Q^{\ddagger}$, cm^3 mol^{-1} $+0.5 \pm 0.5$
$(1/T_{2Q}^b)_0^{264}$, s^{-1} [b]	8930 ± 190 (8865, 8995)	$(1/T_{2Q}^b)_0^{266}$, s^{-1} [b] 4390 ± 56
$(1/T_2^b)_0^{271}$, s^{-1} [b]	$11\,700 \pm 300$ (11 735, 11 601)	$(1/T_2^b)_0^{281}$, s^{-1} [b] 6963 ± 92

[a] $\Delta V_Q^{\ddagger}$ was fixed during the fitting procedure. [b] The percentage of the quadrupolar $(1/T_{2Q}^b)_0$ and kinetic $(k)_0$ contribution to $(1/T_2^b)_0$ was fixed during the fitting procedure (taken from the variable-temperature study at atmospheric pressure).

Table 13. Comparison of Kinetic Results for Water Exchange

	k_{ex}^{298}, s^{-1}	$\Delta H^{\ddagger}$, kJ mol^{-1}	$\Delta S^{\ddagger}$, J K^{-1} mol^{-1}	$\Delta V^{\ddagger}$, cm^3 mol^{-1}	mechanism	ref
$[Cp^*Co(bpy)(H_2O)]^{2+}$	0.60[a]	70.5 ± 4.0[b]	-6 ± 10[b]		$I_{(d)}$	this work
$[Cp^*Rh(bpy)(H_2O)]^{2+}$	1.59×10^3 [a]	47.9 ± 3.0[b]	-18 ± 12[b]		$I_{(d)}$	this work
$[Cp^*Ir(bpy)(H_2O)]^{2+}$	2.19×10^2 [a]	59.1 ± 3.5[b]	4 ± 10[b]		$I_{(d)}$	this work
$[L^2Ru(bpy)(H_2O)]^{2+}$	6.8×10^{-2} [a]	67.5 ± 3.5[b]	-31 ± 14[b]		$I_{(d)}$	this work
$[L^3Ru(bpy)(H_2O)]^{2+}$	8.5×10^{-2} [a]	66.4 ± 3.5[b]	-33 ± 14[b]		$I_{(d)}$	this work
$[L^4Ru(bpy)(H_2O)]^{2+}$	10.2×10^{-2} [a]	65.7 ± 3.5[b]	-34 ± 14[b]		$I_{(d)}$	this work
$[Cp^*Co(H_2O)_3]^{2+}$	60[c]					this work
$[Cp^*Rh(H_2O)_3]^{2+}$	1.6×10^5	65.6 ± 7	$+75.3 \pm 24$	$+0.6 \pm 0.6$	$I_{(d)}$	this work
$[Cp^*Ir(H_2O)_3]^{2+}$	2.53×10^4	54.9 ± 3	$+23.6 \pm 8$	$+2.4 \pm 0.5$	$I_{(d)}$	this work
$[Rh(H_2O)_6]^{3+}$	2.2×10^{-9}	131 ± 23	$+29 \pm 69$	-4.2 ± 0.6	I_a	29
$[Ru(H_2O)_6]^{2+}$	1.8×10^{-2}	88 ± 4	$+16 \pm 15$	-0.4 ± 0.7	I	4
$[Ru(H_2O)_6]^{3+}$	3.5×10^{-6}	90 ± 4	-48 ± 14	-8 ± 2	I_a	4
$[L^2Ru(H_2O)_3]^{2+}$	11.5	76 ± 4	$+30 \pm 11$	$+1.5 \pm 0.4$	$I_{(d)}$	5
$[L^2Os(H_2O)_3]^{2+}$	11.8	66 ± 2	-5 ± 6	$+2.9 \pm 0.6$	$I_{(d)}$	5
$[Ru(CH_3CN)_6]^{2+}$	8.9 ± 10^{-11}	140.3 ± 2.0	$+33.3 \pm 6$	$+0.4 \pm 0.6$	I	4
$[CpRu(CH_3CN)_3]^{+}$	5.6	86.5 ± 2.0	59.6 ± 7.0	11.1 ± 0.5	D	6
$[L^2Ru(CH_3CN)_3]^{2+}$	4.07 ± 10^{-5}	102.5 ± 5.0	15.0 ± 14.0	2.4 ± 0.8	I	6
$[Co(NH_3)_5(H_2O)]^{3+}$	5.7×10^{-6}	111.3 ± 1	$+28 \pm 4$	$+1.2 \pm 0.2$	I_d	30
$[Co(CH_3NH_2)_5(H_2O)]^{3+}$	7.0×10^{-4}	99.0 ± 6	$+26.7 \pm 22$	$+5.7 \pm 0.2$	I_d	35
$[Rh(NH_3)_5(H_2O)]^{3+}$	8.6×10^{-6}	103.0 ± 1	$+3 \pm 5$	-4.1 ± 0.4	I_a	31
$[Rh(CH_3NH_2)_5(H_2O)]^{3+}$	1.06×10^{-5}	112.7 ± 2	$+37.8 \pm 6$	$+1.2 \pm 1.1$	I_d	35
$[Ir(NH_3)_5(H_2O)]^{3+}$	6.1×10^{-8}	118 ± 1	$+11 \pm 4$	-3.2 ± 0.1	I_a	32

[a] As obtained on the basis of the approximation $k_{ex} \approx k_i$(average) from anation studies (see Table 9 and Discussion). [b] As obtained from the temperature dependence of rate constant k_i for the anation of $[LM(bpy)(H_2O)]^{2+}$ with TU (see Table 10). [c] Estimated from the ratio k_{ex}(Co):k_{ex}(Rh):k_{ex}(Ir) (see eq 16) for the anation of $[Cp^*M(bpy)(H_2O)]^{2+}$ (see Discussion).

of water substitution varies very significantly though with the metal M. From the mechanistic point of view, the kinetic results obtained (see Table 9) point to the operation of an I_d mechanism in all of the systems studied. Main support for this comes from the fact that the experimentally obtained second-order rate constant, k_X, after appropriate correction for outer-sphere complex formation (see ref 18 and Table 9), leads to first-order rate constants k_i ($=k_X/K_{os}$) for the interchange step (see eq 9), which are only little affected by the nature of the entering ligand X.[26] For the complex $[Cp^*Co(bpy)(H_2O)]^{2+}$, for example, k_i spans from 0.875 s^{-1} (X = SCN$^-$) to 0.250 s^{-1} (X = Me-im), which leads to a k_i(average) of 0.60 ± 0.29 s^{-1}. The situation is similar for the other complexes (see Table 9), so that the values for k_i(average) can be taken as reasonably good approximations for the rates of M−OH$_2$ bond breaking. The I_d mechanism implies[28] that $k_i \approx k_{ex}$, with k_{ex} being the rate constant for water exchange. This means that k_i(average) is an approximate value for k_{ex}.

As summarized in Table 13, the three homologous complexes $[Cp^*M(bpy)(H_2O)]^{2+}$ (M = Co, Rh, Ir) differ in k_{ex} ($=k_i$(average)) considerably, the relative order being described by (16). It should be pointed out that this substantial rate effect

$$k_{ex}(Co):k_{ex}(Rh):k_{ex}(Ir) = 1:2650:365 \qquad (16)$$

of homologous d^6 metal centers refers to complexes which have the same overall charge and the same ligand field. The comparison of k_{ex} values for $[L^2Ru(bpy)(H_2O)]^{2+}$ and $[Cp^*Rh(bpy)(H_2O)]^{2+}$ corresponds to the comparison of the two isoelectronic low-spin d^6 metal centers Ru(II) and Rh(III), which are comparable in size. They are surrounded by different ligand fields, generating the same overall charge of 2+ though. The substitution of benzene (=L^2) and Ru(II) for the pentamethylcyclopentadienyl anion Cp* (=L^1) and Rh(III) reduces the rate of water exchange by a factor of 2.3×10^4, which demonstrates the enormous rate effect of the anionic ligand Cp*. The fact that the k_{ex} values are similar in magnitude for the three ruthenium complexes $[LRu(bpy)(H_2O)]^{2+}$ with L = L^2, L^3, and L^4 suggests that the ligand field strengths of benzene, cymene, and hexamethylbenzene are rather similar, which is in line with the similar vis spectra of $[L^{2-4}Ru(bpy)(H_2O)]^{2+}$ (see Table 5).

It follows from the kinetic data obtained for the water exchange in the half-sandwich triaqua complexes $[Cp^*M(H_2O)_3]^{2+}$ (M = Rh, Ir) that, at 298 K, the rhodium complex exchanges by a factor of 6.3 faster than the iridium complex (see Table 13). This is very close to the factor of 7.3 resulting for the ratio $k_{ex}(Rh)/k_{ex}(Ir)$ for the water exchange in $[Cp^*M(bpy)(H_2O)]^{2+}$. The absolute rates are very different though, the water exchange in $[Cp^*Rh(H_2O)_3]^{2+}$ being approximately 100 times faster than that in $[Cp^*Rh(bpy)(H_2O)]^{2+}$. This means that the replacement of two water molecules in $[Cp^*Rh(H_2O)_3]^{2+}$ by the bidentate ligand bpy reduces the mobility of the residual water molecule considerably. On the basis of the

(26) The most characteristic feature of a substitution with an associative mode of activation is the strong influence of the nature of the entering ligand on the rate. Nucleophilic substitution in *trans*-$[Pt(py)_2Cl_2]$, which follows an A mechanism, is by a factor of 3750 faster for TU than for N_3^-.[27] The fact that in the present study the k_i values for the reactions of TU and N_3^- with $[Cp^*M(bpy)(H_2O)]^{2+}$ (M = Rh, Ir) differ by less than a factor of 2 (see Table 9) clearly rules out substantial "associative" contributions to the activation process.

(27) See ref 3b, p 236.
(28) See ref 3b, pp 211−212.
(29) Laurenczy, G.; Rapaport, I.; Zbinden, D.; Merbach, A. E. *Magn. Reson. Chem.* **1991**, *29*, 845.
(30) Hunt, H. R.; Taube, H. *J. Am. Chem. Soc.* **1958**, *80*, 2642.
(31) Swaddle, T. W.; Stranks, D. R. *J. Am. Chem. Soc.* **1972**, *94*, 8357.
(32) Tong, S. B.; Swaddle, T. W. *Inorg. Chem.* **1974**, *13*, 1538.

order of reactivity given by (16), one can extrapolate $k_{ex}^{298} \approx 60\ s^{-1}$ for the unstable and hitherto kinetically not studied cobalt species $[Cp^*Co(H_2O)_3]^{2+}$. The volumes of activation for the water exchanges in $[Cp^*Rh(H_2O)_3]^{2+}$ and $[Cp^*Ir(H_2O)_3]^{2+}$ are found to be +0.6 and +2.4 $cm^3\ mol^{-1}$, respectively, and the entropies of activation are +75.3 and +23.6 $J\ K^{-1}\ mol^{-1}$, respectively. These data, especially the volumes of activation, do not provide direct support for the operation of the I_d mechanism. For another low-spin d^6 complex, $Ru(H_2O)_6^{2+}$, the rate constants k_i for the interchange step of complex formation with a variety of entering ligands are also very similar, but with an activation volume for water exchange of $-0.4 \pm 0.6\ cm^3\ mol^{-1}$. The operation of an I_d mechanism was suggested, and the zero value of the activation volume was explained by a competition between a positive contribution due to the loss of a water molecule and a negative one due to the contraction around the small d^6 ion in the transition state.[33] So, in conclusion, the sum of the experimental findings of the present study favors the interpretation that the anation of the species $[LM(bpy)(H_2O)]^{2+}$ (M = Co, Rh, Ir, Ru) and the water exchange in these species and in the triaqua species $[Cp^*M(H_2O)_3]^{2+}$ (M = Rh, Ir) follow an interchange mechanism with M−O(water) bond breaking being rate-controlling.

It is interesting and informative to compare the results of the present study with earlier ones (see Table 13).[34] The introduction of benzene (=L^2) into $[Ru(H_2O)_6]^{2+}$ ($[Ru(H_2O)_6]^{2+} \rightarrow [L^2Ru(H_2O)_3]^{2+}$) enhances the rate of water exchange by a factor of about 640, whereas additional introduction of the ligand bpy ($[L^2Ru(H_2O)_3]^{2+} \rightarrow [L^2Ru(bpy)(H_2O)]^{2+}$) reduces it by a factor of 174, so that water exchange is only by a factor of 3.8 faster in $[L^2Ru(bpy)(H_2O)]^{2+}$ than in the hexaaqua Ru^{2+} ion. Analogously, the couple $[L^2Ru(CH_3CN)_3]^{2+}/[Ru(CH_3CN)_6]^{2+}$ differs in k_{ex} by a factor 4.6×10^5. The most dramatic acceleration of solvent exchange is observed, however, when the Cp or Cp* ligand is introduced. $[CpRu(CH_3CN)_3]^+$ exchanges acetonitrile 6.3×10^{10} times faster than $[Ru(CH_3CN)_6]^{2+}$,[6] and for the water exchange of the couple $[Cp^*Rh(H_2O)_3]^{2+}/[Rh(H_2O)_6]^{3+}$ it is even the factor 7.3×10^{13}. The k_{ex} data obtained for the homologous species $[M(RNH_2)_5(H_2O)]^{3+}$ (M = Co, Rh, Ir; R = H, CH_3) are interesting in a twofold sense.[35] They prove, on the one hand, that the rate of water exchange is not at all governed by the size of the metal. On the other hand, a shift to more positive volumes of activation is observed for complexes with bulkier spectator groups. Clearly, the crowding around the metal center causes the mechanism to be shifted toward a more dissociatively activated position in the $I_a \leftrightarrow I_d$ mechanistic continuum, and for an I_d mechanism the rate constants increase with the bulkiness of the spectator group. These steric effects however are smaller than electronic effects. The ligand field in $[M(RNH_2)_5(H_2O)]^{3+}$, comprising five σ-donating ligands, has a much less metal-specific effect on k_{ex} than the ligand field in $[Cp^*M(bpy)(H_2O)]^{2+}$, comprising the σ-donating/π-accepting ligands Cp* and bpy.

As pointed out by Ludi et al.,[6] the most remarkable increase in coordinated solvent lability observed for π-arene acetonitrile and π-arene aqua cations is most probably due to several effects. The interaction of transition metal cations with σ-donors/π-acceptors such as benzene, Cp^-, and Cp^{*-} leads to a metal-specific delocalization of the overall charge. In addition, the residual coordinated solvent molecules are subject to a trans influence (affecting bond lengths) as well as to a kinetic trans effect (affecting the ease of transition state formation). The 2 orders of magnitude decrease in the water exchange rate observed upon replacing two water molecules by bpy in $[Cp^*M(H_2O)_3]^{2+}$ is the opposite of what is expected for an I_d mechanism for increased steric crowding at the metal center. It can be explained by a smaller trans effect due to the fact that both ligands, Cp* and bpy, compete for the d^6 metal orbitals. To fully analyze and separate the effects of charge delocalization, trans influence and trans effect, more systematic structural and kinetic studies have to be carried out. It might also be helpful to approach the system from the theoretical side by calculating the metal-specific geometry, charge distribution, and bond strengths in the transition state of the dissociative interchange step.

Conclusions

The results detail earlier findings concerning the lability of coordinated water molecules in π-arene aqua complexes of transition metal cations. As described by (17) for a given metal

$$[M(H_2O)_6] \ll [LM(H_2O)_3] > [LM(bpy)(H_2O)] \quad (17)$$

M such as Co, Rh, Ir, or Ru (charges omitted), the introduction of π-arene ligands L such as benzene or cyclopentadienyl ion into hexaaqua cations $[M(H_2O)_6]^{3+}$ increases the lability of the three residual water molecules drastically. This effect is most pronounced for the anionic ligands L = Cp* and Cp and less pronounced for neutral ligands L such as benzene, cymene, and hexamethylbenzene. Additional introduction of 2,2′-bipyridine reduces the lability of the water molecule in $[LM(bpy)(H_2O)]$ by about 2 orders of magnitude. For $[Cp^*M(bpy)(H_2O)]^{2+}$ there is a strong metal effect on the lability of the coordinated water, following the order Co ≪ Rh > Ir. Obviously, the pK_a of the coordinated water does not correlate with its kinetic lability.

The anation according to (18) is a second-order process, with a rate constant k_X, which, after correction for outer-sphere

$$[LM(bpy)(H_2O)]^{2+} + X \xrightarrow{k_X} [LM(bpy)X]^{2+} + H_2O \quad (18)$$

complexation, is a good measure for the rate of water exchange. The mechanism of (18) and of water exchange according to (19) with M = Rh, Ir is of the interchange type ($I_{(d)}$).

$$[Cp^*M(H_2O)_3]^{2+} + 3H_2O^* \xrightarrow{k_{ex}} [Cp^*M(H_2O^*)_3]^{2+} + 3H_2O \quad (19)$$

Acknowledgment. Sponsorship of this work by the Deutsche Forschungsgemeinschaft, Swiss National Science Foundation (Grant 20-39483.93), Verband der Chemischen Industrie e.v., and Otto-Röhm-Stiftung is gratefully acknowledged. The authors thank Dr. Pierre-André Pittet for useful discussions.

Supplementary Material Available: Tables SI−SIX, listing complete crystallographic data, calculated coordinates of hydrogens, distances and angles, and thermal parameters, and Tables SX−XII, listing NMR relaxation rates and quadrupolar and kinetic contributions (18 pages). Ordering information is given on any current masthead page.

IC940646Q

(33) Aebischer, N.; Laurenczy, G.; Ludi, A.; Merbach, A. E. *Inorg. Chem.* **1993**, *32*, 2810.

(34) The experimentally determined k_{ex} values are the rate constants for the exchange of a particular coordinated water molecule of the first coordination sphere. The rate constant for the exchange of an unspecified water molecule is *n* times greater, where *n* is the number of water molecules in the first coordination sphere.

(35) González, G.; Moullet, B.; Martinez, M.; Merbach, A. E. *Inorg. Chem.*, in press.